# FREQUENCY FACTOR OF THE SEMIEMPIRICAL MODEL FOR THE RADIATION-INDUCED CONDUCTIVITY IN SPACECRAFT POLYMERS

**Andrey Tyutnev, Vladimir Saenko, Evgenii Pozhidaev**

National Research University Higher School of Economics, 20 Myasnitskaya Ulitsa, 101000, Moscow, Russia
*Email:* aptyutnev@yandex.ru

***Abstract.*** **We have extended the existing Rose-Fowler-Vaisberg model of the radiation-induced conductivity in polymers by incorporating the latest ideas borrowed from theoretical and experimental results obtained in the field of electronic transport in molecularly doped polymers. These include the Poole-Frenkel type field dependent mobility and the arguments of the dipolar disorder formalism based on the Gaussian disorder model. Theory validation uses a new experimental technique based on the electron-gun technology allowing combined induced conductivity and carrier mobility measurements in a typical molecularly doped polymer. Quasi-band and hopping theories of the carrier transport are critically discussed.**

***Keywords: electrons, polymers, model calculations, spacecraft application***

## 1. INTRODUCTION

Knowing the radiation induced conductivity (RIC) of dielectrics is essential for estimation of the electric fields emerging in these materials under space environment and as such is of great interest to the spacecraft charging community. To interpret the vast volume of the accumulated experimental data, we have developed an advanced semi- empirical model of RIC based on the concept of the multiple trapping quasi-band theory incorporating relevant radiation chemistry results. This model has become known as the Rose-Fowler-Vaisberg (RFV) model [1].

Equations of the RFV model are as follows:

$$\begin{cases} \dfrac{dN}{dt} = g_0 - k_r N_0 N, \\ \dfrac{\partial \rho}{\partial t} = k_c N_0 \left[ \dfrac{M_0}{E_1} \exp\left(-\dfrac{E}{E_1}\right) - \rho \right] - \nu_0 \exp\left(-\dfrac{E}{kT}\right) \rho, \\ N = N_0 + \int_0^\infty \rho dE. \end{cases} \quad (1)$$

Usually, at $t = 0$ $N_0(t)$ and $\rho(E,t)$ are assumed to be both zero.

By definition, RIC is equal to $\gamma_r(t) = e\mu_0 N_0(t)$, where $e$ is an elementary electric charge. Thus, system (1) refers to a unipolar (for convenience, electron) conduction and is effectively a Cauchy time-dependent problem with no spatial dependence .

Here $N(t)$ is the total concentration of excess electrons (equal to the concentration of immobile holes, which act as recombination centers). $N_0(t)$ is the concentration of mobile electrons in extended states (in transfer band) with microscopic mobility $\mu_0$; $g_0$ is the generation rate of free charge carriers (assumed constant during irradiation); $k_r$ – the recombination coefficient of mobile electrons with localized holes; $k_c$ is the trapping rate constant; $M_0$ is the total concentration of traps exponentially distributed in energy ( $E$ is positive and is taken downwards from the energy level of the transport band); $E_1$ is the parameter of the trap distribution; $T$ is the temperature; $\rho(E,t)$ is the time dependent density distribution of trapped electrons; $\nu_0$ is the frequency factor and $k$ is the Boltzmann's constant. Dispersive parameter $\alpha$ , which defines the major temporal features of the transient curves, equals the ratio $kT / E_1$. Also, $\tau_0 = (k_c M_0)^{-1}$ is the lifetime of mobile electrons before trapping.

RIC generally consists of two components, the prompt $\gamma_p$ and the delayed $\gamma_d$ one. The former obeys a first order kinetics with a time constant in the subnanosecond range so that for irradiations longer than 1 ns it strictly repeats the pulse shape scaling with the dose rate. In the RFV model, the latter is found by solving Eqs. (1) and using the relationship

$$\gamma_d = \gamma_r - g_0 \mu_0 \tau_0 e \quad (2)$$

The prompt component should be inferred from experiment since the one given by the RFV model $\widehat{\gamma}_p = g_0 \mu_0 \tau_0 e$ usually differs markedly from its true value.

Determination of the RFV parameters is based on a comparison of model predictions with experimental data. The best analysis of this model belongs to Arkhipov and Rudenko [2, 3] and refers to the small as well as large

signal regimes, including pulsed and step-function irradiations. Model parameters are not unique. In fact, it is known that in all analytical expressions $\mu_0$ and $\tau_0$ appear only as a product. This feature still holds for the Langevin mechanism of the bimolecular recombination, which stipulates that

$$k_r = k_{rL} = (e/\varepsilon\varepsilon_0)\mu_0$$

Here, $\varepsilon$ is the relative permittivity of a polymer and $\varepsilon_0$ is the electrical constant. An asymptotic ($\nu_0 t \gg 1$) current build-up and decay in a small signal step-function irradiation is uniquely defined even by a triple product $\mu_0\tau_0\nu_0^{\alpha}$.

In this situation, it is important to have an experimental technique which allows direct evaluation of the frequency factor $\nu_0$. The aim of this article is to test such a technique and discuss the problems it entails.

## 2. BASIC CONSIDERATIONS

To assess the frequency factor, we compare experimental and computed decaying currents in the near post pulse region ($t > t_p$, where $t_p$ is the length of the radiation pulse). All numerical calculations have been done using the MathCad packet working with the analytical formulas developed by Arkhipov [3] employing the famous $\tau$ -function approximation applicable for $\alpha \leq 0.5$.

In our case, the solution of Eqs. (1) looks like:

$$j_{rd}(t) = g_0 e\left[q(t) - \mu_0\tau_0 F\right], \quad \text{if} \quad t \leq t_p$$

and

$$j_{rd}(t) = g_0 e\left[q(t) - q(t - t_p)\right], \quad \text{if} \quad t \geq t_p$$

Here, $q(t) = \mu_0 F \tau(t)$

and $\tau(t) = \tau_0 (\nu_0 t)^{\alpha} \alpha^{-1}\gamma^{-1}(\alpha, \nu_0 t)$.

Also, $\gamma(\alpha, x) = \int_0^x x^{\alpha-1}\exp(-x)dx$ is an incomplete gamma-function (in MathCad packet used in this work, it is given by $\Gamma(\alpha)\,pgamma(x,\alpha)$).

Fig. 1 shows computed results illustrating the limitations of such an approach for $t_p$ = 20 $\mu$ s. The straightforward interpretation is possible when the decaying current exhibits a plateau (we call it an effective mobility plateau [4, 5]) whose duration is close to the inverse frequency factor (see curves *1* and *2* on the figure). In this case, the prompt component $\gamma_p$ as given by Eq. 2 by far exceeds the delayed one during an irradiation pulse. An interesting situation arises when a decay pattern transforms into a straight line $j \propto t^{-0.6}$ (curve *4*) in which case a relationship $\nu_0 t_p \approx 4$ holds. As frequency factor gets larger and larger, the amplitude of the decaying current at the pulse end progressively increases but its decay shape tends to become almost universal. To find $j_{rd}$ at the pulse end, we had to apply Eq. 2 as now the prompt component constitutes only a small part of the RIC and gets even smaller as the frequency factor continues to rise.

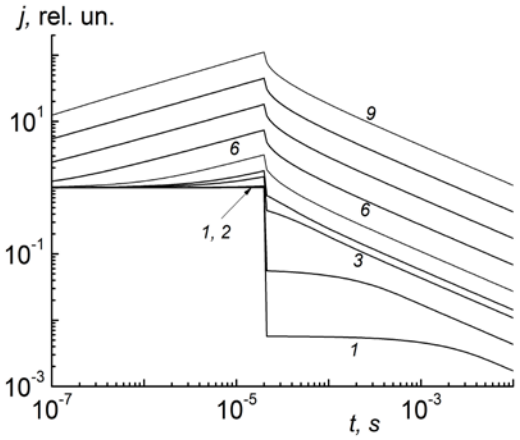


*Figure 1. Calculated RIC curves (in units of the prompt component) for various values of $\nu_0 = 10^3$ (1), $10^4$ (2), $10^5$ (3), $2\times 10^5$ (4), $10^6$ (5), $10^7$ (6), $10^8$ (7), $10^8$ (8 )and $10^{10}$ $s^{-1}$(9). For all curves $\alpha = 0.4$.*

Implementing this approach needs knowledge of the dispersion parameter $\alpha$ and a current decay shape factor to judge the proximity between experimental and computed curves. We chose it to be a ratio $B = j_{rd}(t_p)/j_{rd}$ (100 $\mu$ s). To find $\alpha$, we approximated the current decay in the time interval 0.1-1 ms by a power law $j \propto t^{-\beta_1}$ assuming that $\alpha = 1\text{-}\beta_1$. Table 1 gives the computed values of $j_{rd}(t_p)$ and $B$ for $\alpha$ = 0.4 and different $\nu_0$ obtained by processing curves presented on Fig. 1.

Experimentally, such an approach is not easy to realize as it should involve high-intensity electron pulses of nanosecond duration [4]. One might try to relax this demand by using moderately strong 20 microsecond rectangular pulses. The main limitation of such an approach is its inability to distinguish current decay shape for large frequency factors. But even the lower limit of the frequency factor may be important.

**Table 1.** Computed values of $j_{rd}(t_p)$ given in units of the RIC prompt component which is independent of $\nu_0$

| $\nu_0$, $s^{-1}$ | $j_{rd}(t_p)$. | $B$ |
|---|---|---|
| $10^3$ | $5.6\cdot 10^{-3}$ | 1.02 |
| $10^4$ | $5.5\cdot 10^{-2}$ | 1.18 |
| $10^5$ | 0.46 | 2.50 |
| $2\cdot 10^5$ | 0.80 | 3.95 |
| $10^6$ | 2.13 | 4.56 |
| $10^7$ | 6.4 | 5.47 |
| $10^8$ | 17.1 | 5.80 |
| $10^9$ | 43.8 | 5.92 |
| $10^{10}$ | 110 | 5.92 |

Careful examination of data presented in Tab. 1 allows drawing some important conclusions about behavior of the RIC delayed component. As $\nu_0$ increases, $j_{rd}(t_p)$ rises as well. Initially, there is a linear relationship between them ($10^3$-$10^4$ $s^{-1}$) which transforms into an asymptotic law $j_{rd}(t_p) \propto \nu_0^{0.4}$ for $\nu_0$ exceeding $10^8$ $s^{-1}$ when $\nu_0 t_p \geq 2000$. This corresponds to the increase of $j_{rd}(t_p)$ by a factor of 2.51 for $\nu_0$ rising by an order of magnitude as data in the second column in Tab. 1 demonstrates.

As for direct evaluation of the frequency factor and its plausible field dependence, the best chance to succed involves analyzing decay RIC currents featuring plateaus or degenerating into a straight line $j_{rd} \propto t^{-1+\alpha}$ (naturally in logarithmic scale) as curves *1 – 4* on Fig.1 demonstrate.

Working with concave curves whose slopes progressively increase as we approach the pulse end from the right involves very accurate analysis and often completely fails at high fields as curves *6-8* graphically demonstrate. Such curves become virtually indistinguishable as far as their form is concerned (shape parameter $B$ almost coincides as the last column in Table 1 shows).

Below we apply this approach to evaluate the RFV frequency factor and to study its field dependence in some commercial polymers including a model disordered solid extensively investigated by our group recently.

## 3. EXPERIMENTAL RESULTS

Investigated polymers include commercial films of Kapton (25 $\mu$m thick) and its Russian analogue PM-1-OA (10 $\mu$ m), Teflon-FEP (25 $\mu$ m), polyethyleneterephthalate (PET, 12 $\mu$ m), low density polyethylene (LDPE, 20 $\mu$ m), polystyrene (PS, Styroflex, 20 $\mu$ m) and a molecularly doped polycarbonate (30% DEH:PC, 10 $\mu$ m ) all supplied with Al electrodes 32 mm in diameter. These were irradiated by 20 $\mu$s rectangular pulses of 50 keV electrons inside a vacuum chamber of the ELA-65 electron gun at room temperature. Electric field could be changed from 1 to 100 V/$\mu$m, the average dose rate being typically $3\cdot 10^5$ Gy/s so that a dose per pulse did not exceed about 6 Gy. The radiation pulse had 0.7 $\mu$s rise time and 0.25 $\mu$s fall time with a flat top 19 $\mu$s long. Depth distribution of the dose rate was slightly non-uniform with an average dose rate being typically 1.6 times larger than at the front surface of a sample.

Registration time was limited to 1 ms only due to an extremely small time constant RC = 0.1 $\mu$s (load resistance 100 $\Omega$ with a sample capacitance smaller than 2000 pF) and a very high recording rate of 10 MHz. Experiments have been done in a small signal regime when RIC response is linear in dose rate, allowing us to characterize it as referring to a unit dose rate: $K_p$, $K_{rd}(t_p)$ or $K_{rd}(t')$ for the prompt and delayed components, the last two quantities referring to the pulse end or the time $t'$ after it (Tab. 2).

Polymers tested clearly fall into two groups: one with a dominating prompt component allowing easy determination of the delayed current at the pulse end (Teflon-FEP, LDPE) and the others in which separating these components presents great difficulty even at moderate fields (Fig. 2). In this case and especially at the highest fields used (Fig. 3), the separation procedure drew heavily on the published data for nanosecond irradiations characterizing the prompt RIC of polymers with high accuracy [4]. Comparing Figs. 2 and 3, we note how strongly an electric field affects $j_{rd}(t_p)$ in all polymers except LDPE and Teflon-FEP (see Tab. 2).

Table 2. List of investigated polymers and their RIC parameters

| Polymer | $\nu_0 \times 10^{-6}$, $s^{-1}$ | $\beta_1$ | $B$ | $K_p \times 10^{15}$ (SI units) | $K_{rd}(t_p) \times 10^{15}$ (SI units) | $\kappa$ |
|---|---|---|---|---|---|---|
| Teflon-FEP | 0.3 | 0.95 | 4.5 | 2.7 | 0.4 | 0.2 |
| LDPE | 0.5 | 0.45 | 3.8 | 6 | 1.5-2.55 | 0.31 |
| Kapton | 500 | 0.93 | 23 | 3.5 | 5.5-15 | 0.6 |
| PM-1-OA | | 0.78 | 7.3 | 0.8 | 3.6-40 | 0.6-1.5 |
| PET | 1 | 0.95 | 12.7 | $\leq 1$ | 5.4-42 | 0.6-1.1 |
| PS | 2 | 0.8 | 9.2 | 3 | 5.7-21 | 0.7-1 |
| 30% DEH:PC | $10^5$ | 0.3 | 2.2 | 3 | 3-82 | 1-1.7 |

***Note***. *$K_p$ and $K_{rd}(t_p)$ are given in SI units ($\Omega^{-1}$ $m^{-1}Gy^{-1}s$) while $K_{rd}(t_p)$ and $\kappa$ are indicated at a field range from 10 V/ $\mu$ m to a maximum value presented on Figs. 3 and 4. Data for Teflon-FEP refers to 40 V/ $\mu$ m only.*

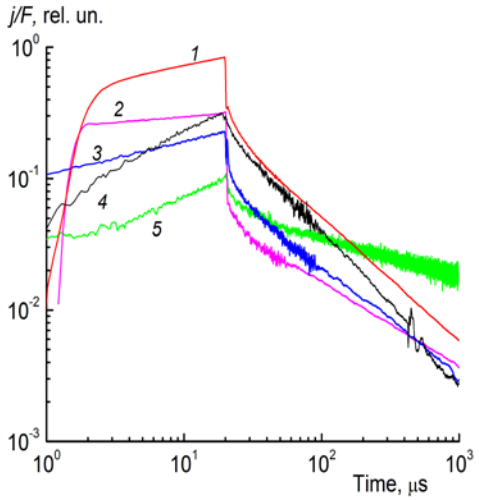


*Figure 2. RIC current densities per unit electric field measured at a fixed dose rate $3\times10^5$ Gy/s (pulse length 20 $\mu$ s). Polymers tested: PS (1), LDPE (2), PM-1OA (3), PET (4) and 30% DEH:PC (5). Electric field 20 V/ $\mu$ m.*

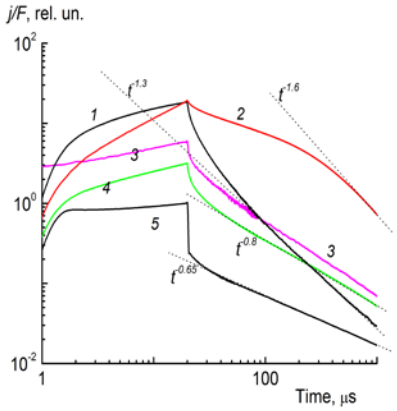


*Figure 3. RIC current densities per unit electric field measured at a fixed dose rate ($3\times10^5$ Gy/s) for a pulse length 20 $\mu$ s. Polymers tested: PET (1), 30% DEH:PC (2), PS (3), PM-1OA (4), and LDPE (5). Maximum electric field 60 (PS, LDPE) and 100 V/ $\mu$ m (PET, PM-1OA, 30% DEH:PC).*

To characterize the field dependence of the RIC delayed component, we introduce an exponent $\kappa$ figuring out in the following relationship

$$K_{rd}(t_p) \propto F^{\kappa} \quad (\kappa = d \lg K_{rd}(t_p) / d \lg F) \qquad (3)$$

Last two columns in Tab. 2 contain data for $j_{rd}(t_p)$ and $\kappa$ measured at the lowest and the highest electric fields used which are as follows (in V/ $\mu$ m): Teflon-FEP (40), Kapton (10-40), PS and LDPE (20-60), PM-1OA, PET and 30% DEH:PC (1-100). This data are detailed on Fig. 4. We emphasize that the prompt component of RIC simply scales with an electric field .

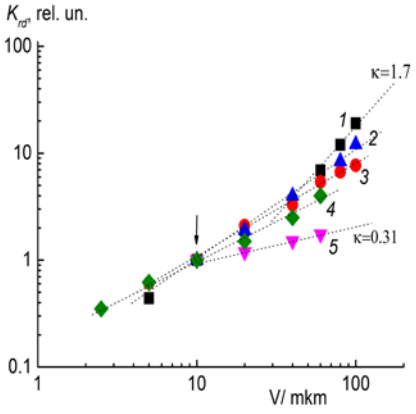


*Figure 4. Field dependence of $K_{rd}$ measured at 10 $\mu$ s after the pulse end. Polymers tested: 30% DEH:PC (1), PM-1OA (2), PET (3), PS (4) and LDPE (5). An arrow indicates the standard electric field used.*

Now, we have made an attempt to evaluate the corresponding frequency factors and their possible field dependence. For this purpose, we combined data from Figs. 2 and 3 in such a way as to plot pairs of curves for each polymer measured at the extreme fields (mentioned above) making $j_{rd}(t_p)$ to coincide (Fig. 5).

In each pair of curves the one denoted by *1* refers to the lowest
field.

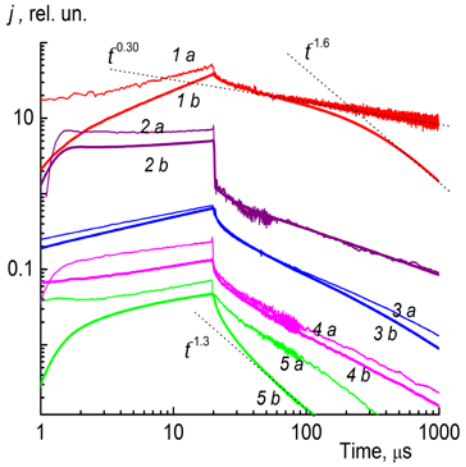


*Figure 5. RIC current densities measured for a fixed dose rate ($3\times10^5$ Gy/s) for a pulse length 20 $\mu$ s grouped in pairs for the lowest (a) and the highest (b) electric field (for different polymers curves are not to scale). The curves were made to coincide just after the pulse end (so that their delayed components were equal). Polymers tested: 30% DEH:PC (1), LDPE (2), PM-1OA (3), PS (4) and PET (5) for pairs of fields 20 and 100 (1, 3, 5) and 20 and 60 V/ $\mu$ m (2, 4).*

The most simple interpretation offers itself for LDPE. Its $\alpha \approx 0.45$ and $B = 3.8$ favor $\nu_0 = 5\times10^5$ s$^{-1}$. As both decay curves coincide, we conclude that there is no field effect on the frequency factor. In PM-1OA and PS a small but progressively increasing field effect is showing itself up. The observed divergence of decay curves in 30% DEH:PC should be ascribed to the transit time effects in full accord with the published data [6].

Strong field effects in PET are also partly due to possible crossing of the sample by a small group of charge carriers as already previously observed [7]. We see that values of the frequency factor in all polymers except Kapton and 30% DEH:PC are rather low. The reasons for such results will be discussed below.

The data presented on Fig. 4 deserve some consideration since as we will see below it is closely related to the field dependence of the frequency factor which so far evaded reliable identification. Tab. 2 and Fig. 4 show that $\kappa$ may reach 1.5 and even 1.7 which means that the current density $j_{rd}(t_p)$ or $j_{rd}(t')$ varies as $F^{2.5}$ or $F^{2.7}$ (even faster than the quadratic field dependence). And this fact runs into serious contradiction with the currently accepted explanation based on the Onsager theory of the field-assisted thermal dissociation of the geminate ion pairs [8, 9].

## 4. DISCUSSION

The Onsager theory predicts that the pair separation probability is given by the formula [10]

$$\Omega_\infty = \exp\left\{\frac{r_c}{r_0}\cdot\frac{[\exp(-\varsigma)-1]}{\varsigma}\right\} \qquad (4)$$

where the Onsager radius $r_c = e^2/(4\pi\varepsilon\varepsilon_0 kT)$, $\varsigma = eFr_0/kT$ and $r_0$ is the electron-hole separation in a geminate pair. A very useful parameter characterizing the field dependence of $\Omega_\infty$ is $\xi = d\ln\Omega_\infty / d\ln F$ which is similar to parameter $\kappa$ introduced earlier (see Eq. 3). As $F$ rises from 1 to 100 V/ $\mu$ m, $\xi$ increases from about 0.3 to a maximum $\xi_m$ (which is very sensitive to $F$ ) at about 10 V/ $\mu$ m rapidly falling afterwards.

According to the traditional approach, the delayed component of the RIC is proportional to $\Omega_\infty$ and as a result, is expected to follow the field dependence of it, so that $K_{rd}(t) \propto F^{\xi}$ . On the other hand, an experimentally found field dependence of the RIC delayed component obeys a similar functional law with yet another exponent $\kappa$ (see Eq. 3). Field effects in these two exponents are quite different even on the qualitative level: whereas $\xi$ shows a non-monotonic behavior passing through a maximum at about 10 V/ $\mu$ m approaching zero on both sides away from it, parameter $\kappa$ steadily increases as the field rises from 1 to 100 V/ $\mu$ m at least in 30% DEH:PC, PM-1OA and PET.

In the traditional field range used to investigate RIC field effects (1-40 V/ $\mu$ m) these differences are difficult to discern and the Onsager theory has been used universally for interpreting the experimental results. The discrepancy shows up only at high electric fields exceeding approximately 60 V/ $\mu$ m as encountered in the present work. To underline this discrepancy, we compared the field dependence of $\kappa$ and $\xi$ using our experimental data for 30% DEH:PC and the computed

results given by Eq. 4 for $r_c$ = 19.2 nm ($\varepsilon$ = 3.0, $T$ = 290 K) and $r_0$ = 6 nm (Fig. 6).

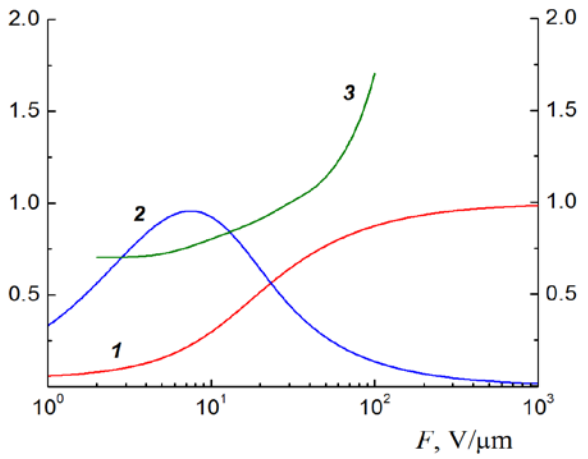


*Figure 6. Computed values of $\Omega_\infty$ (1), $\xi$ (2) and an experimental $\kappa$ (3) for 30% DEH:PC plotted as a function of the electric field.*

As Fig. 6 shows the field variation of $\xi$ and $\kappa$ is rather close at moderate fields (5-20 V/$\mu$m) but gets diametrically opposite at high fields: whereas the former starts rapid decreasing, the latter continues to rise. One is forced to conclude that some other factor comes into operation increasing RIC additionally to the traditional Onsager mechanism.

Based on mobility studies in molecularly doped polymers generally [6] and on our extensive work with 30% DEH:PC in particular [12], we claim that such a factor is the frequency factor as we suggested earlier in [11].

Time of flight measurements in this molecularly doped polymer revealed that hole drift mobility exhibited a strong Poole-Frenkel type field dependence ( $\mu \propto \exp(\beta_{PF} F^{1/2})$ with $\beta_{PF}$ = 0.39 ($\mu$m/V)$^{1/2}$ covering the field range from 1 to 100 $\mu$V/m [12]. Not all, but the most part of this field dependence applies to the frequency factor and thus shows up in Formula (3). The same situation exists in PM-1OA and PET and is expected to appear in PS and Kapton at 100 V/$\mu$m, not reached in our studies.

These two mechanisms (the Onsager theory and the Poole-Frenkel mobility field effect) act independently, so that their combined effect is given by the product

$$K_{rd}(t) \propto F^{\xi+\delta} \qquad (5)$$

where $\delta$ approximates as a power law the above discussed contribution of the Poole-Frenkel mobility field dependence so that we have the relation $\kappa = \xi + \delta$

This result explains the fact that the current-voltage characteristic does not saturate at high fields. Indeed, though $\xi \to 0$ as $F \to \infty$, the second exponent $\kappa$ may even continue to rise. But then the question arises as to why did we fail to see these changes in the frequency factor in experiments (Fig. 5) specifically designed to observe them directly? The answer is closely related to the persisting dilemma of the prevailing charge transport mechanism in polymers: quasi-band versus hopping one. In the first case, carrier transport occurs via conducting states accompanied by multiple trapping and de-trapping events while in the second, it involves only the localized hopping sites.

This dilemma on the theoretical front looks like the confrontation of the multiple trapping theory (the RFV model included) and the hopping formulations, among them the Gaussian disorder model [6] and the correlated dipolar glass model [13] are the most popular. Unlike the former, the latter models lead to substantially larger values of the frequency factor ($10^9$ to $10^{12}$ s$^{-1}$) as opposed to much smaller $\nu_0$ (typically about $10^5$-$10^7$ s$^{-1}$). For example, the published values of it in 30% DEH:PC are around $10^{11}$ s$^{-1}$ at 5 V/$\mu$m [14]. The dipolar disorder formalism of Borsenberger and Bässler based on the Gaussian disorder hopping model fully supports such an assertion [6]. This observation resolves the controversy with the molecularly doped polymer tested. The same argumentation apparently applies to PS, PM-1OA and PET which are expected to feature the hopping conduction, especially PS whose benzene rings are perfect candidates for the hole hopping centers.

The case of LDPE deserves special attention. Indeed, it allows direct estimation of the frequency factor since $\alpha$ may be assumed to be 0.5 so that $\nu_0 \approx 5 \times 10^5$ s$^{-1}$. It is important that there are time resolved RIC measurements done with a 10-fold shorter pulse duration (2 $\mu$s), which allowed direct estimation of $\nu_0$ from the duration of the initial mobility plateau (about ten microseconds long) [15]. In this situation any field induced changes of this parameter could be immediately detected. But this polymer, as ill luck would have it, displays only a mild field dependence of $K_{rd}$ (Fig. 4) which makes any detection attempt doomed to failure in accord with experimental results.

At last, we encounter strong field effects in PET (Fig. 6) but values of $\beta_1$ (1.25 and 2.2 at 10 and 100 V/ $\mu$ m respectively) exceeding unity testify to the presence of transit effects for a group of carriers as indicated earlier in our paper [7]. But unlike the case of 30% DEH:PC, the current decay immediately after pulse end defies any reasonable explanation.

## 5. CONCLUSIONS

We have conducted RIC studies in a number of polymers using 20 $\mu$ s rectangular pulses of 50 keV electrons in a wide range of electric fields (10 to 60 or even 100 V/ $\mu$ m) concentrating mainly on the behavior of the delayed component (field dependence and decay pattern after the pulse end). The field dependence of $K_{rd}(t)$ at strong fields ($\geq$ 60 V/ $\mu$ m) contradicts the traditional Onsager theory of the field-assisted thermal generation of free charge carriers. To overcome this discrepancy, we introduced the field dependence of the frequency factor in terms of the RFV model. All attempts to securely estimate the expected field induced changes using existing analytical formulas have failed. We interpret this result as an indication of $\nu_0$ being much higher than hitherto assumed. Accommodating this fact would require some readjustment of the existing values of the product $\mu_0\tau_0$, decreasing it to some extent.

## 6. REFERENCES


1. Tyutnev, A.P., Saenko, V.S.,. Pozhidaev, E.D. & Ikhsanov, R.Sh. (2015). Experimental and theoretical studies of radiaton-induced conductivity in spacecraft polymers. *IEEE Trans. Plasma Sci*. 43(9), 2915-2924.
2. Rudenko A. I., & Arkhipov, V. I. (1982). Drift and diffsion in materials with traps. III. Analysis of transient current and transit time characteristics. *Phil. Mag. B* . 45(2) , 209-226.
3. Arkhipov V. I. (1993). An idiabatic model of trap-controlled dispersive transport and recombination. *J. Non-Cryst. Solids*, 163, 274-282.
4. Tyutnev, A.P., Abramov, V.N., Dubenskov, P.I., Saenko, V.S., Vannikov, A.V. & Pozhidaev, E.D. (1986). Time-resolved nanosecond radiation-induced conductivity in polymers. *Acta Polymerica*, 37, 336-342.
5. Tyutnev, A.P., Sadovnichii, D.N. & Boev, S.G. (1995). The effective mobility of excess charge carriers in disordered matrices. *Chem. Phys. Repts*. 13(8-9), 1367-1385.
6. Borsenberger, P.M. & Weiss D.S. (1998). Organic photoreceptors, Marcel Dekker, New York.
7. Tyutnev, A.P., Kundina, Yu. F., Saenko, V.S., Doronin, A.N. & Pozhidaev, E.D. (2001). Radiation-induced conductivity of PET: theoretical model and its applications. *High Perform. Polym.*. 13, 493-504.
8. Hummel, A. (1974). Ionization in nonpolar molecular liquids by high energy electrons. *Adv. Rad. Chem*. 4, 1-102.
9. Freeman, G. R. (Ed.) (1987). Kinetics of nonhomogeneous processes. New York-Chichester: J. Wiley & Sons.
10. Hong, K.M. & Noolandi, J. (1978). Solution of the time-dependent Onsager problem. *J. Chem. Phys*. 695026-5039.
11. Tyutnev, A. P., Ikhsanov, R. Sh., Saenko V. S. & Pozhidaev, E. D. (2012). Analysis of the carrier transport in molecularly doped polymers using the multiple trapping model with the Gaussian trap distribution. *Chem. Phys.*, 404, 88-93.
12. Schein, L.B., Saenko, V. S., Pozhidaev, E. D., Tyutnev, A. P. & Weiss D.S. (2009). Transient conductivity measurements in a molecularly doped polymer over wide dynamic ranges. *J. Phys. Chem. C.*, 113, 1067-1073.
13. Novikov, S. V., Dunlap, D. H., Kenkre, V. M., Parris P. E. & Vannikov, A. V. (1998). Essential role of correlations in governing charge transport in disordered organic materials. *Phys. Rev. Lett.*, 81, 4472-4475.
14. Tyutnev, A. P., Weiss, D. S., Dunlap D. H. & Saenko, V.S. (2014). Time of flight current shapes in molecularly doped polymers: effects of sample thickness and irradiation side and carrier generation width. *J. Phys. Chem. C.*, 118, 5150-5158, .
15. Tyutnev, A.P. & Sadovnichii, D.N. (1998). Field effects in charge carrier effective mobility in polymers. *Khim. Phyz.*, 17(3), 121-133, (in Russian).